# Al-Powered Bayesian Inference

Sean O'Hagan\* and Veronika Ročková<sup>†</sup> April 2, 2025

#### Abstract

The advent of Generative Artificial Intelligence (GAI) has heralded an inflection point that has changed how society thinks about knowledge acquisition. While GAI cannot be fully trusted for decision-making, it may still provide valuable information that can be integrated into a decision pipeline. Rather than seeing the lack of certitude and inherent randomness of GAI as a problem, we view it as an opportunity. Indeed, variable answers to given prompts can be leveraged to construct a prior distribution which reflects assuredness of AI predictions. This prior distribution may be combined with tailored datasets for a fully Bayesian analysis with an AI-driven prior. In this paper, we explore such a possibility within a non-parametric Bayesian framework. The basic idea consists of assigning a Dirichlet process prior distribution on the data-generating distribution with AI generative model as its baseline. Hyperparameters of the prior can be tuned out-of-sample to assess the informativeness of the AI prior. Posterior simulation is achieved by computing a suitably randomized functional on an augmented data that consists of observed (labeled) data as well as fake data whose labels have been imputed using AI. This strategy can be parallelized and rapidly produces iid samples from the posterior by optimization as opposed to sampling from conditionals. Our method enables (predictive) inference and uncertainty quantification leveraging AI predictions in a coherent probabilistic manner.

Keywords: Dirichlet Process Prior, Imaginary Data, Non-parametric Bayes

<sup>\*</sup>Sean O'Hagan is a 4th year PhD student at the Department of Statistics of the University of Chicago.

†Veronika Ročková is the Bruce Lindsay Professor of Econometrics and Statistics in the Wallman Society of Fellows at the Booth School of Business at the University of Chicago. The author would like to thank Tijana Zrnic for pointing out a reference to catalytic priors which was a catalyst for this research. This research was supported by the NSF (DMS: 1944740).

### 1 Introduction

Due to its ability to synthesize information from various sources, Generative Artificial Intelligence (GAI) is quickly becoming the source of knowledge for many of its users. However, the practical utility of GAI models largely depends on the user's understanding of their mechanistic (probabilistic) properties. Generative models simply produce stochastic responses to prompts, with the level of randomness influenced by both the prompt's specificity and the AI's ability and confidence in providing an accurate answer. This inherent randomness raises questions about the extent to which important decisions can be based on a single AI output answer. We argue that the variability in the answers themselves offers an opportunity to generate (a) a random prior guess at the correct answer, and (b) probabilistic predictions via AI-induced distributions obtained by repeated prompting. While our society has resisted surrendering important decision-making to artificial intelligence, AI predictive systems may serve as a useful primer for further analysis. This work explores the possibility of articulating prior information through AI data augmentation for a fully Bayesian analysis.

Our setup consists of independent labeled data  $\mathcal{D}_n = \{(Y_i, \mathbf{X}_i)\}_{i=1}^n$  which are tailored to a specific question regarding a parameter of interest  $\theta_0$ . For example, we will later analyze a dermatology dataset where the label is one of six distinct but closely overlapping skin conditions within the group of Erythemato-Squamous Diseases (ESDs) [36]. While the parameter of interest  $\theta_0$  may index a statistical model (including deep learning models involving high-dimensional  $\theta_0$ ), we regard it more generally as a minimizer of a certain loss function [5]. Our goal is to understand how generative AI can be used for prior elicitation to conduct fully Bayesian inference on  $\theta_0$  as well as predictive inference on  $Y_i^*$  given  $X_i^* \notin \mathcal{D}_n$ .

This work is based on the premise that generative models produce synthetic data which can be converted into (informative) priors. The idea of using imaginary training data for prior construction is nearly as old as Bayesian statistics itself, dating to at least Laplace in the 18th century [17]. In the context of Bayes factor model comparisons, intrinsic priors [4] result from converting an improper uninformative prior into a proper posterior on a sample of a "minimal" training size. Arithmetic and geometric mean aggregates

of Bayes factors under all plausible training data subsets approximately correspond to a Bayes factor under the so-called "intrinsic prior". The expected-posterior prior [32] is a special case which results from averaging posterior distributions, given imaginary data, over all imaginary data arising from a suitable predictive measure (for example predictive distribution under a simpler model or empirical distribution of the observed data). Besides intrinsic and expected-posterior priors, data augmentation ideas for prior constructions for model determination have been explored by many others, including [16, 25, 33] or [31]. We are not necessarily concerned with objective prior elicitation for model selection but rather with subjective prior articulation for actual inference about  $\theta_0$  under one posited model.

Only very few priors have had as much practical and theoretical impact as the Zellner's g-prior [38]. Motivated by imaginary data, this prior adopts the covariance structure from observed data to facilitate conjugate analysis in normal regression. Inspired by [10], [7, 20] propose predictive elicitation of a proper conjugate prior for generalized linear models based on observable quantities (historical data) which serve as a prior guess at observable outcomes. Similar data augmentation (DA) priors, that have the same form as the likelihood, have also been studied by [3] who considered a broader class of conditional mean priors arguing that it is easier to elicit prior information on means of observables rather than on regression coefficients. Related ideas occurred in specialized contexts including proportional hazards regression [18]. A more recent incarnation of DA priors is the catalytic prior [19] that involves simulated data from a posterior predictive distribution under a simpler (donor) model trained on  $\mathcal{D}_n$ . The catalytic prior is then constructed from the, suitably down-weighted, fake training samples so that it is conjugate with the posited model. While the catalytic prior appears conceptually related to the expected-posterior prior [14, 15, 27, 32] as well as power-priors [7], but it originates from a different set of desiderata. With complex models and small datasets, likelihood-based analysis can be unstable or infeasible and may be enriched by augmenting the observed data with imaginary data generated from a posterior predictive under a simpler model [19, 27]. This results in a posterior distribution that is pulled towards the posterior under the simpler model, resulting in estimates and predictions with potentially better properties. Our work

has been motivated by catalytic priors in the sense that we also view generative AI as a posterior predictive simulator but we approach AI prior articulation differently. First, we use simulations from generative AI models trained on massive dataset that are different from the proprietary observed data  $\mathcal{D}_n$ . Catalytic priors use simulations from posterior predictive distributions under models trained on  $\mathcal{D}_n$ , inherently using  $\mathcal{D}_n$  twice. Second, we consider a non-parametric Bayesian inference framework by constructing a prior for  $F_0$ , the distribution function underlying independent realizations inside  $\mathcal{D}_n$ , as opposed to a prior on  $\theta_0$ . Shifting focus from inference on an unknown parameter  $\theta_0$  to inference on an unknown data-generating distribution  $F_0$  allows harnessing generative AI output in a more transparent way. Indeed, generative AI can be leveraged to produces imaginary data  $\mathcal{D}_m^* = \{(Y_i^*, \boldsymbol{X}_i^*)\}_{i=1}^m$  which could be regarded as samples from the prior on  $F_0$ . We align with [7] who state that "it is easier to think of observable quantities when eliciting priors, rather than specifying priors for regression parameters directly, since parameters are always unobserved." However, unlike [7], we focus directly on non-parametric inference on  $F_0$  which obviates the need to commit to a particular model and breaks the precarious codependence between the (conjugate) prior and the model.

Our idea is extremely simple. We view generative AI as a base distribution for a Dirichlet process prior on  $F_0$  [11]. Inference on  $\theta_0$  can be accomplished through the loss-based posterior framework of [5, 6, 26] where the parameter of interest  $\theta_0$  is a functional of  $F_0$ . The Dirichlet process prior admits an embarrassingly parallel posterior bootstrap algorithm [13, 26] that generates independent and exact samples from the nonparametric posterior distribution over the data-generating process. Since the AI prior on  $\theta_0$  is defined only implicitly through an AI prior on  $F_0$ , Markov chain Monte Carlo (MCMC) analysis that relies on sampling from conditionals is not immediately unavailable. Instead of obtaining dependent samples using MCMC, we obtain independent posterior samples by optimization of suitably randomized objective functions along the lines of [13]. This strategy allows us to obtain posterior distributions of functionals as well as posterior predictive distributions. These distributions can be used to report (predictive) uncertainty in optimization-based

<sup>&</sup>lt;sup>1</sup>This reference was pointed out to one of the authors by Tijana Zrnic during her visit at Booth.

machine learning techniques (such as random forests or deep learning) for which uncertainty quantification has been challenging or unavailable. Our work has been inspired by the prediction-powered inference framework [1, 22, 39] for constructing valid confidence intervals and p-values that allows for AI systems to be used for data augmentation. The prediction-powered inference (PPI) framework posits estimators for minimizers of convex objectives that leverage predictions from a black-box AI model on additional unlabeled data in order to aid estimation. PPI does this by making use of a rectifier which relates AI prediction error to bias and employing a strategy reminiscent of de-biasing. Our work can be viewed as a Bayesian counterpart to this framework.

The paper is structured as follows. In Section 2 we review various prior elicitation methods using AI data augmentation in likelihood-driven Bayesian inference. Section 3 presents AI prior elicitation in loss-function driven Bayesian inference. Section 4 presents theory and hyper-parameter calibration strategies. Section 5 shows two real data applications including AI-assisted disease diagnosis and astrophysics. Section 6 wraps up with a discussion.

### 2 AI-Powered Bayesian Inference

Suppose that we observe labeled data  $\mathcal{D}_n = \{(Y_i, \mathbf{X}_i)\}_{i=1}^n$  and want to perform a supervised analysis involving a parameter of interest  $\theta_0 \in \Theta \subseteq \mathbb{R}^d$  as well as predictive inference about  $Y_{new}$  given  $\mathbf{X}_{new} = \mathbf{x}_{new}$  where  $(Y_{new}, \mathbf{X}_{new}) \notin \mathcal{D}_n$ . In addition to observations  $\mathcal{D}_n$ , we have access to a (stochastic) black-box predictive model  $\hat{\mu}_{AI}(\mathbf{x})$  which generates random labels  $\tilde{Y}_i = \hat{\mu}_{AI}(\mathbf{x})$  when prompted by  $\mathbf{x}$ . One can regard  $\hat{\mu}_{AI}(\mathbf{x})$  as an implicit simulator from a predictive distribution of a complex model (e.g. a large language model underlying generative AI) trained on massive data  $\mathcal{D}_{AI}$  that is unavailable to the user and different from  $\mathcal{D}_n$ .

To conduct predictive inference, a Bayesian forecaster would typically issue a posterior predictive distribution

$$\pi(Y_{new} \mid \boldsymbol{x}_{new}, \mathcal{D}_n) = \int \pi(Y_{new} \mid \boldsymbol{x}_{new}, \theta) \pi(\theta \mid \mathcal{D}_n) d\theta$$
 (2.1)

based on the posterior distribution of  $\theta$  given  $\mathcal{D}_n$ 

$$\pi(\theta \mid \mathcal{D}_n) \propto \pi(\theta) \pi(\mathcal{D}_n \mid \theta)$$

under a postulated model  $\pi(\mathcal{D}_n \mid \theta)$  and a chosen prior  $\pi(\theta)$ . There are two conundrums that have given a pause to some practitioners before fully embracing Bayesian inference: (1) the specification of the prior  $\pi(\theta)$ , and (2) the specification of the model, e.g.  $\pi(\mathcal{D}_n \mid \theta) = \prod_{i=1}^n \pi(Y_i \mid \mathbf{X}_i, \theta)$  for independent realizations. While Bayesians have historically faced taunts about (subjective) priors, model choice is far more consequential in a likelihood-based analysis and should be defended at least as fiercely as the prior choice. This work deals with (subjective) prior elicitation based on observable predictions from an AI predictive model. The issue of model specification will be tackled using a non-parametric framework Section 3.2 which allow Statisticians "to remain honest about their ability to perfectly model the data" [26].

In the following three subsections, we present several approaches for AI prior elicitation that could be used in the context of likelihood-driven Bayesian inference. Our main discussion will center around nonparametric Bayesian inference driven by loss function in Section 3.

### 2.1 Likelihood-Driven AI Priors

While the AI model is a black box predictive machine, it implicitly defines a model and a prior if one were willing to assume that  $\hat{\mu}_{AI}(\cdot)$  generates samples from a posterior predictive distribution (2.1) under some label distribution  $\pi_{AI}(Y \mid \boldsymbol{x}, \theta)$ , prior  $\pi_{AI}(\theta)$  and a training model  $\pi(\mathcal{D}_{AI} \mid \theta)$ . This argument might be justifiable from the "prequential" point of view [9] that focuses solely on predictive distributions (as opposed to models and priors) and argues that the quality of an inference method can truly be gauged by the quality of its forecasts. We regard AI forecasts as a potentially useful proxy for the true unobserved outcomes.

One hypothetical (but impossible) strategy of turning AI knowledge into priors would be to utilize  $\pi_{AI}(\theta \mid \mathcal{D}_{AI}) \propto \pi_{AI}(\theta)\pi(\mathcal{D}_{AI} \mid \theta)$  as a prior  $\pi(\theta)$  for the predictive distribution  $\pi(Y_{new} | \boldsymbol{x}_{new}, \mathcal{D}_n)$  based on labeled data  $\mathcal{D}_n$ . However, we cannot directly access the parameter posterior simulator  $\pi_{AI}(\theta \mid \mathcal{D}_{AI})$  from  $\hat{\mu}_{AI}(\cdot)$ . What we can access, however, is imaginary data  $\mathcal{D}_m^* = \{(Y_i^*, \boldsymbol{X}_i^*)\}_{i=1}^m$  consisting of predictive imputations from  $\hat{\mu}_{AI}(\cdot)$ . The idea of turning such imaginary data  $\mathcal{D}_m^*$  into a prior has bountiful rewards and can be approached in various different ways. We explore data augmentation strategies for parametric priors in Section 2.1.1 and for non-parametric priors in Section 3.2. These approaches should be distinguished from martingale posteriors [12] which also leverage predictive imputation for posterior computation but in a very different way. Martingale posteriors are based on large sequences of missing data generated from one-step-ahead predictive distributions that are continuously updated with newly generated data. A posterior distribution over a parameter of interest for exchangeable observations is obtained using the Doob's theorem by computing a functional (such as the mean) of observed data augmented with the imputed sequence. In contrast, we do not consider predictive imputation of an (infinite) sequence of observations from continuously updated posterior predictive. Rather, we perform imputation of a finite number of fake observations from a given "predictive" distribution which does not update with newly generated imaginary data points.

#### 2.1.1 Power AI Priors

We align with the insight by [7] that "it is much easier to elicit information about the typical outcome than to attempt the extremely difficult task of eliciting prior knowledge about  $\theta$ ". Transmitting prior information through data augmentation has a long history in Bayesian statistics [17], Zellner's g-prior being perhaps the most prominent example. If we were to generate fake training data  $\mathcal{D}_m^* = \{(Y_i^*, X_i^*)\}_{i=1}^m$  (using either  $X_i^* = X_i$  or by sampling with replacement from  $X_i$ 's), we can augment  $\mathcal{D}_n$  with  $\mathcal{D}_m^*$  and apply any (Bayesian) procedure on this joint sample under some posited model  $\pi(Y \mid X, \theta)$ . The contribution of imaginary data could be possibly down-played by raising their contribution to the joint likelihood to a small power  $1/\delta > 0$ . This is the basic premise of data-augmentation priors. The power-prior [7, 20] is one of the early examples within the context of generalized linear models, where  $X_j^* = X_j$  for  $1 \leq j \leq m = n$  and where auxiliary labels  $Y_j^*$  serve as a fixed prior

guess at  $Y_j$  given  $\mathbf{X}_j$ . Following [10], [7] construct a conjugate prior by plugging  $\mathcal{D}_m^*$  into the likelihood of an exponential family model assuming that  $Y_j^*$ 's are conditionally independent, given a model parameter  $\theta$ . In addition, each imaginary data point  $Y_j^*$  (given  $\mathbf{X}_j^* = \mathbf{X}_j$ ) is down-weighted by some small parameter  $1/\delta > 0$  and could be interpreted as a prior prediction (or guess) for  $E[Y_j \mid \mathbf{X}_j]$ . Zellner's g-prior is a special case in normal regression where  $g = \delta$ . The construction in [7] is related but different from data-augmentation priors of [3] who allow for m to be different from n and where  $\mathbf{X}_i^*$  is not necessarily one of the  $\mathbf{X}_i$ 's. Moreover, while [7] assign the same weight parameter  $\delta$  to  $Y_j^*$  that acts as an effective prior sample size for the prior, the framework of [3] assigns a weight  $w_j^*$  to each new observation  $(Y_j^*, \mathbf{X}_j^*)$  where  $w_j^*$  can be viewed as a possibly fractional number of observations associated with a particular  $(Y_j^*, \mathbf{X}_j^*)$ . We will see later in Section 3.2 that thinking of  $w_j^*$ 's as random rather than fixed will correspond to a Bayesian bootstrap style strategy.

Power AI priors could be constructed by regarding AI predictions  $Y_j^* = \hat{\mu}_{AI}(\boldsymbol{X}_j^*)$  as arising from the same model  $\pi(Y \mid \boldsymbol{X}, \theta)$  as the data  $\mathcal{D}_n$  using either [7] or [3] as follows:

$$\pi_{Power}(\theta) \propto \prod_{i=1}^{m} \pi(Y_i^* \mid \boldsymbol{X}_i^*, \theta)^{1/\delta} \pi_W(\theta)$$

where  $\pi_W(\theta)$  is some baseline working prior. Power priors could be enhanced by incorporating the randomness in  $\mathcal{D}_m^*$ . Instead of building a prior from one particular realization of  $\mathcal{D}_m^*$ , expected-posterior priors [14, 15, 27, 32] and catalytic priors [19] incorporate randomness of  $\mathcal{D}_m^*$  but do so in different ways. We explain the differences below.

### 2.1.2 Expected-Posterior AI Priors

The expected-posterior AI prior along the lines of Definition 1 in [32] could be constructed as a typical power prior after margining out the imaginary data

$$\pi_{EP}(\theta) \propto \int \prod_{i=1}^{m} \pi(Y_i^* \mid \boldsymbol{X}_i^*, \theta) \pi_W(\theta) \pi_{AI}(\mathcal{D}_m^*) d\mathcal{D}_m^*, \tag{2.2}$$

where  $\pi_{AI}(\cdot)$  consists of first generating prompts  $X^*$  (possibly using observed  $X_j$ 's) and labels  $Y^*$  from the posterior predictive distribution underlying the simulator  $\hat{\mu}(X^*)$  (as discussed at the beginning of Section 2.1). The posterior distribution  $\pi(\theta \mid \mathcal{D}_n)$  under the

prior (2.2) corresponds to a typical joint posterior under the prior  $\pi_W(\theta)$  after averaging out  $\mathcal{D}_m^*$ . Indeed, under the prior (2.2) we have

$$\pi(\theta \mid \mathcal{D}_n) = \int \pi(\theta \mid \mathcal{D}_n, \mathcal{D}_m^*) \pi_{AI}(\mathcal{D}_m^*) d\mathcal{D}_m^*.$$
(2.3)

This characterization has a practical benefit for posterior simulation from (2.3). A Markov chain  $\{\theta^{(t)}\}_{t=1}$  with a stationary distribution (2.3) can be obtained by generating a joint chain  $\{(\theta^{(t)}, \mathcal{D}_m^{*(t)})\}_{t=1}^T$  by first refreshing  $\mathcal{D}_m^*$  from  $\pi_{AI}(\mathcal{D}_m^*)$  at every MCMC iteration and then, given  $\mathcal{D}_m^*$ , generate  $\theta^{(t)}$  from the joint posterior. Marginally,  $\theta^{(t)}$ 's would be distributed according to (2.3). Unlike with power priors, this strategy refreshes the fake data during simulation as opposed to conditioning on them a-priori. A related approach was considered by [27] in the context of exchangeable observations where predictions from a simple donor model, for which prior elicitation was feasible, were transferred to a more complex recipient model through imaginary data. The implications of treating the imaginary data as random as opposed to fixed were explored in [23] in the context of contrastive learning for Bayesian computation using the Metropolis-Hastings algorithm.

### 2.1.3 Catalytic AI Priors

In catalytic priors [19], imaginary data  $\mathcal{D}_m^*$  are generated from a Bayesian predictive distribution under a simple donor model trained on  $\mathcal{D}_n$  for which prior elicitation was easier. The data  $\mathcal{D}_m^*$  are then plugged into a likelihood representing a more complex recipient model whose parameters would be difficult to estimate using only  $\mathcal{D}_n$ . Formally, the catalytic version of an AI prior could be written as

$$\pi_{CAT,m}(\theta) \propto \left(\prod_{i=1}^{m} \pi(Y_i^* \mid \boldsymbol{X}_i^*, \theta)\right)^{\alpha/m} = \exp\left\{\frac{\alpha}{m} \sum_{i=1}^{m} \log \pi(Y_i^* \mid \boldsymbol{X}_i^*, \theta)\right\}$$
(2.4)

for some  $\alpha > 0$  which regulates the influence of the prior and where 1/m performs averaging over the contributions of single imaginary data points  $Y_i^*$ . A similar idea could be implemented using AI predictions. Unlike catalytic priors, however, generating fresh data  $\mathcal{D}_m^*$  from an AI model precludes from the double use of data  $\mathcal{D}_n$ . The practical implementation of Bayesian analysis with catalytic priors (2.4) would entail choosing  $\alpha$  using some

criterion and then simulating very many fake observations m so that the averaging in (2.4) performs satisfactory approximation to Monte Carlo integration. Indeed, as  $m \to \infty$  the prior approaches

$$\pi_{CAT,\infty}(\theta) \propto \exp\left\{\alpha \int \log \pi(Y^* \mid \boldsymbol{X}^*, \theta) \pi_{AI}(Y^*, \boldsymbol{X}^*) d(Y^*, \boldsymbol{X}^*)\right\}.$$
 (2.5)

We highlight an important difference between (2.5) and the expected-posterior prior (2.2). If we denote the unnormalized expressions in (2.5) and (2.2) as  $f_{CAT,\infty}$  and  $f_{EP}$  respectively, then from the Jensen's inequality  $E \log X \leq \log EX$ , the population catalytic prior satisfies  $f_{CAT,\infty}(\theta) \leq f_{EP}(\theta)$  for all  $\theta \in \Theta$ ,  $\alpha \in \mathbb{N}$  with  $m = \alpha$ ,  $\pi_W(\theta) \propto 1$ , and  $\pi_{AI}(\mathcal{D}_m^*) = \prod_{i=1}^m \pi_{AI}(Y_i^*, \mathbf{X}_i^*)$ . The expected-posterior prior is more general and allows for information blending from a larger set of imaginary data that are not necessarily iid. In summary, m in the prior (2.2) actually corresponds to the imaginary data sample size represented by  $\alpha$  in (2.4) with  $m = \infty$ .

While the expected-posterior prior (2.2) allows for exact posterior simulation by updating the fake data at each MCMC simulation step by averaging out uncertainty in  $\mathcal{D}_m^*$ , catalytic priors (2.4) compute a different object due to the Jensen's gap. The population version actually corresponds to posteriors obtained by augmenting a single typical imaginary distribution using estimated moments of  $(Y^*, \mathbf{X}^*)$ . This can be seen, for example, in Gaussian linear regression with unit variance, where the catalytic prior based on simulations  $\mathcal{D}_m^*$  would become

$$\pi_{CAT,m} = N\left(\hat{\theta}, \frac{m}{\alpha} (\boldsymbol{X}^{*'} \boldsymbol{X}^{*})^{-1}\right)$$

where  $\hat{\theta} = (\boldsymbol{X}^{*'}\boldsymbol{X}^{*})^{-1}\boldsymbol{X}^{*'}\boldsymbol{Y}^{*}$ . If we choose  $\boldsymbol{X}^{*} = \boldsymbol{X}$  where only the labels  $Y_{i}^{*}$  are subject to predictive imputation, this corresponds to the g-prior with  $g = m/\alpha$ . The population catalytic prior would then become  $N(\theta^{*}, \frac{1}{\alpha}\Sigma_{X}^{-1})$ , where  $\Sigma_{X} = \lim_{m \to \infty} \frac{1}{m}\boldsymbol{X}^{*'}\boldsymbol{X}^{*}$  and  $\theta^{*} = \Sigma_{X}^{-1}c$ , where  $c = \lim_{m \to \infty} \frac{1}{m}\boldsymbol{X}^{*'}\boldsymbol{Y}^{*}$ . While the population catalytic prior plugs moments into the Gaussian prior, the expected-posterior prior is a Gaussian mixture

$$\int N\left(\hat{\theta}, \frac{m}{\tau} (\boldsymbol{X}^{*'} \boldsymbol{X}^{*})^{-1}\right) \pi_{AI}(\mathcal{D}_{m}^{*}) d\mathcal{D}_{m}^{*}.$$

All of the prior constructions in Section 2.1.1, 2.1.2 and 2.1.3 force the observed data  $\mathcal{D}_n$  and AI-generated data  $\mathcal{D}_m^*$  into a conjugate relationship. This prescription is much stronger

than just assuming that the model is well-specified because it demands that the prior has arrived from the very same model. We prefer avoiding the double mis-specification (model and the prior) and will therefore focus on a non-parametric Bayesian analysis based on AI-informed priors on  $F_0$  as opposed to  $\theta_0$ .

## 3 Bayes without the Likelihood

Instead of assuming that there exists  $\theta_0$  such that the observed data  $\mathcal{D}_n$  has been independently realized from  $\pi(Y \mid \boldsymbol{X}, \theta_0)$ , we adopt a non-parametric viewpoint, where the  $\mathcal{D}_n$  arrives from an iid experiment involving an unknown distribution function  $F_0$  for  $(Y, \boldsymbol{X})$ . Similarly as in [5, 26], we shift focus from  $\theta_0$  to  $F_0$ . The question of prior elicitation will be tackled by converting observable predictions from an AI model into non-parametric priors on  $F_0$ . Suppose that the unknown parameter  $\theta_0$  is a solution to the optimization problem

$$\theta_0(F_0) = \arg\min_{\theta} \int \ell(\theta, Y, \boldsymbol{X}) dF_0[(Y, \boldsymbol{X})], \tag{3.1}$$

where  $\ell(\theta, Y, \mathbf{X})$  is a loss function and  $F_0$  is the unknown distribution for  $(Y, \mathbf{X})$ . The parameter of interest is not necessarily tied to a statistical model and is defined more generally as a minimizer of a population loss under an unknown sampling distribution  $F_0$ . This parameter may correspond to an actual parameter of a statistical model if one takes  $\ell(\theta, Y, \mathbf{X}) = -\log \pi(Y \mid \mathbf{X}, \theta)$ .

### 3.1 Gibbs AI Priors

Bissiri et al. [5] formalized a framework for coherent probabilistic updating of prior beliefs  $\pi(\theta)$  about  $\theta_0$  from observations  $\mathcal{D}_n$  through a functional  $\pi_{GP}(\theta | \mathcal{D}_n) \propto \pi(\theta) \exp\left[-w\ell_n(\theta, \mathcal{D}_n)\right]$ , where  $\ell_n(\theta, \mathcal{D}_n) \equiv \frac{1}{n} \sum_{i=1}^n \ell(\theta, Y_i, \boldsymbol{X}_i)$  and where w > 0 is referred to as a learning rate. This so-called "Gibbs posterior" corresponds to the actual posterior when  $\ell(\theta, Y, \boldsymbol{X}) = -\log \pi(Y | \boldsymbol{X}, \theta)$ . Similarly as in the likelihood-driven power AI priors from Section (2.1.1), we can incorporate  $\mathcal{D}_m^*$  through

$$\pi_{GP}(\theta) \propto \pi_W(\theta) \exp\left[-\alpha \ell_m(\theta, \mathcal{D}_m^*)\right]$$
 (3.2)

for some working prior  $\pi_W(\cdot)$  and a learning rate  $\alpha > 0$ . Similarly as in Section 2.1.2, one could consider an expected Gibbs posterior prior version where the data  $\mathcal{D}_m^*$  is marginalized out. Due to the coherency, the Gibbs posterior under the "Gibbs prior" (3.2) writes as

$$\pi_{GP}(\theta \mid \mathcal{D}_n, \mathcal{D}_m^*) \propto \pi_W(\theta) \exp\left[-w \,\ell_n(\theta, \mathcal{D}_n) - \alpha \,\ell_m(\theta, \mathcal{D}_m^*)\right].$$
 (3.3)

When r = n/m for some r > 0, i.e.  $m \to \infty$  as  $n \to \infty$ , and under suitable regularity conditions on  $\ell(\cdot)$  (see e.g. [8] or supplemental material of [26]) the Gibbs posterior has the following asymptotic normal distribution as  $n \to \infty$ 

$$\sqrt{n(1+1/r)}\left(\theta - \widehat{\theta}_{n,m}^{\alpha}\right) \to z \sim \mathcal{N}(0, [wJ_1(\theta_0) + \alpha J_2(\theta_0)]^{-1}),$$

where

$$J_1(\theta) = \int \nabla^2 \ell(\theta, Y, \boldsymbol{X}) dF_0[(Y, \boldsymbol{X})] \quad \text{and} \quad J_2(\theta) = \int \nabla^2 \ell(\theta, Y, \boldsymbol{X}) dF_{AI}[(Y, \boldsymbol{X})] \quad (3.4)$$

where

$$\widehat{\theta}_{n,m}^{\alpha} = \arg\min\{w \,\ell_n(\theta, \mathcal{D}_n) + \alpha \,\ell_m(\theta, \mathcal{D}_m^*)\}$$
(3.5)

is a potentially biased estimator of  $\theta_0$ . This result can be shown by simple adaptation of general Gibbs posterior theory developed earlier in [8]. While the Gibbs posterior (3.3) can be a useful inferential object, simulating from it using MCMC can be at least as challenging as simulating from regular posteriors (see [30] and references therein). We consider a related, but computationally far more feasible, strategy that performs simulation through optimization of randomized objectives. Such strategies have proven useful in various contexts including high-dimensional variable selection [29].

## 3.2 Non-parametric AI Priors

Rather than expressing prior beliefs about  $\theta_0$  defined in (3.1) through  $\pi(\cdot)$ , we can express them through a prior  $\pi(F)$  on  $F_0$ . This will lead to a procedure that is related conceptually but computationally quite different compared to MCMC sampling from (3.3). Since the sampling distribution  $F_0$  is unknown, we can place a Dirichlet process (DP) prior with an AI base prior as follows

$$F \sim DP(\alpha, F_{AI}),$$
 (3.6)

where  $\alpha > 0$  is the usual concentration parameter and  $F_{AI}$  is the base measure which can only be accessed though its simulations  $(Y_i^*, \mathbf{X}_i^*)$ .

#### 3.2.1 AI Base Measure

Denote the density of this base distribution as  $f_{AI}(Y^*, X^*)$  and factorize it into

$$f_{AI}(Y^*, \mathbf{X}^*) = f_{AI}^X(\mathbf{X}^*) \times f_{AI}^Y(Y^* \mid \mathbf{X}^*).$$

The density  $f_{AI}^X(\boldsymbol{X}^*)$  can be viewed as a distribution over prompts. For our practical illustrations, we will assume that it is based on the observed covariates, i.e.  $f_{AI}^X(\boldsymbol{X}^*) = \sum_{i=1}^n g_i \delta_{\boldsymbol{X}_i}$  for some (fixed or random) weights  $g_i > 0$  such that  $\sum_{i=1}^n g_i = 1$ . Given the prompt  $\boldsymbol{X}^*$ , the density  $f_{AI}^Y(Y^* | \boldsymbol{X}^*)$  is defined implicitly by the AI generator  $\hat{\mu}(\boldsymbol{X}^*)$ , be it ChatGPT or any other black-box predictive model. Perhaps the simplest way to construct  $f_{AI}^Y(Y^* | \boldsymbol{X}^*)$  would be an empirical distribution of this historical data, i.e.  $f_{AI}^Y(Y^* | \boldsymbol{X}^*) = \frac{1}{m} \sum_{j=1}^m \delta_{(Y_j^*, \boldsymbol{X}_j^*)}$ , where  $\mathcal{D}_m^* = \{(Y_j^*, \boldsymbol{X}_j^*)\}_{j=1}^m$  have been generated hierarchically from  $\boldsymbol{X}_j^* \sim f_{AI}^X$  and then  $Y_j^* = \hat{\mu}(\boldsymbol{X}_j^*)$ . Using the log-likelihood loss function, this strategy is closely related to the power priors discussed in Section 2.1.1 that treat the historical observations as fixed. Just like with posterior-expected priors from Section 2.1.2, however, it might be desirable to incorporate randomness in  $\mathcal{D}_m^*$  and treat  $f_{AI}$  (or at least  $f_{AI}^Y$ ) as a continuous density. From the properties of the DP prior [35], as  $n \to \infty$  asymptotic consistency of the posterior (3.7) is achieved under certain regularity conditions regardless of the choice of  $F_{AI}$  [26].

### 3.2.2 Posterior Bootstrap

The prior distribution on  $\theta$  is implied by a prior distribution on F in (3.6) using the mapping (3.1) where

$$\theta \sim \underset{\theta'}{\operatorname{arg\,min}} \int \ell(\theta', Y, \boldsymbol{X}) dF[(Y, \boldsymbol{X})] \quad \text{for} \quad F \sim DP(\alpha, F_{AI}).$$

From the conjugacy of the DP process, we see that having observed  $\mathcal{D}_n$ , the posterior on F satisfies  $F \mid \mathcal{D}_n \sim DP(\alpha + n, G_n)$  where  $G_n = \frac{\alpha}{\alpha + n} F_{AI} + \frac{1}{\alpha + n} \sum_{i=1}^n \delta_{Y_i, X_i}$ . The non-parametric

### Algorithm 1 Posterior Bootstrap

**Require:** Input observed data  $\mathcal{D}_n$ , concentration  $\alpha > 0$  and approximation truncation m.

- 1: for  $t \leftarrow 1$  to B do
- 2: Draw imaginary data  $\mathcal{D}_m^* = \{(Y_i, \boldsymbol{X}_i^*)\}_{i=1}^m$  from  $f_{AI}$  defined in Section 3.2.1.
- 3: Draw weights  $(w_{1:n}^{(t)}, w_{1:m}^{*(t)})$  from  $Dir(1, \ldots, 1, \alpha/m, \ldots, \alpha/m)$ .
- 4: Compute  $\theta^{(t)}$  from (3.8).
- 5: **return** Posterior Bootstrap sample  $\{\theta^{(t)}\}_{t=1}^{B}$ .

posterior on  $\theta$  can be then computed [13] simply by taking a functional of samples F from its posterior using

$$\theta \sim \underset{\theta'}{\operatorname{arg\,min}} \int \ell(\theta', Y, \boldsymbol{X}) dF[(Y, \boldsymbol{X})] \quad \text{for} \quad F \sim DP(\alpha + n, G_n).$$
 (3.7)

With an empirical AI base measure based on historical data  $\mathcal{D}_m^*$ , the  $t^{th}$  posterior sample  $\theta^{(t)}$  can be simply computed as

$$\theta^{(t)} = \arg\min_{\theta'} \left[ \sum_{i=1}^{n} w_j^{(t)} \ell(\theta, Y_i, \mathbf{X}_i) + \sum_{j=1}^{m} w_j^{*(t)} \ell(\theta, Y_j^*, \mathbf{X}_j^*) \right]$$
(3.8)

where  $w_j^{(t)}$  and  $w_j^{*(t)}$  are DP-posterior implied weights whose refreshment induces a posterior for  $\theta$ . With a continuous base prior  $f_{AI}^Y$  for the labels  $Y^*$ , the second sum in (3.8) is infinite and approximate computation is required. One possibility is to perform approximate sampling from the DP posterior using the Posterior Bootstrap Algorithm (Algorithm 2 in [13] outlined in Algorithm 1). The idea is to assign a random weight to each observation in  $\mathcal{D}_n$  and  $\mathcal{D}_m^*$  perform repeated optimization of the randomized objective through (3.8). The posterior distribution is induced by uncertainty in F and, since  $\theta$  is a functional of F, we can obtain posterior distribution for a wider class of parameters  $\theta$  than possible within a classical likelihood-based Bayesian analysis [6]. This could be viewed as one possible Bayesian approach to M-estimation.

Having obtained samples  $\{\theta^{(t)}\}_{t=1}^{B}$  through optimization over a dataset consisting of observed and fake labeled data, we can proceed with inference (uncertainty quantification) on  $\theta_0$  defined in (3.1) or posterior predictive inference as follows. For a likelihood-based

loss function  $\ell(\theta, Y, \mathbf{X}) = -\log \pi(Y \mid \mathbf{X}, \theta)$ , the predictive distribution for  $Y_{new}$  given  $X_{new}$  could be computed though (2.1) as

$$\pi(Y_{new} \mid \boldsymbol{X}_{new}) = \frac{1}{B} \sum_{t=1}^{B} \pi(Y \mid \boldsymbol{X}, \boldsymbol{\theta}^{(t)}).$$

For example, predicting  $Y_{new} \in \{1, ... C\}$  from  $\mathbf{X}_{new}$  using a deep learning (DL) classification model with class probabilities  $f_{\theta}(\cdot) \equiv [f_{\theta}^{1}(\cdot), ..., f_{\theta}^{C}(\cdot)]$  parametrized by DL weights  $\theta$ , we could obtain the non-parametric posterior for  $f_{\theta}$  under the AI prior using Posterior Bootstrap. The predictive distribution of  $P[Y_{new} = c \mid \mathbf{X}_{new}, \mathcal{D}_n]$  for the new label would then be the posterior-averaged class probability  $\frac{1}{B} \sum_{t=1}^{B} f_{\theta^{(t)}}^{c}(\mathbf{X}_{new})$ .

The practical utility of the bootstrap posterior for inference on  $\theta_0$  can be gauged from its asymptotic distribution.

### 4 Theory

Consider data  $Y_1, \ldots, Y_n \sim F_0$  and a base measure  $F_{AI}$ . If  $F_{AI}$  is a mixture of m point masses, we denote these by  $Y_1^*, \ldots, Y_m^*$ . Otherwise, we let  $Y_1^*, \ldots, Y_m^* \sim F_{AI}$  for some suitably large m as in the posterior bootstrap algorithm. Since we are considering asymptotic behavior, we let  $\alpha$  depend on n and fix  $\alpha = \gamma n$  for some constant  $\gamma > 0$ . We define the oracle risk minimizer

$$\theta_0^{\gamma} = \arg\min_{\theta} \int \ell(\theta, Y) \, dF_0(Y) + \gamma \int \ell(\theta, Y) \, dF_{AI}(Y) \,. \tag{4.1}$$

noting its dependence on  $\gamma$ . Similarly, we define the empirical risk minimizer

$$\widehat{\theta}_n^{\alpha} = \arg\min_{\theta} \sum_{i=1}^n \ell(\theta, Y_i) + \frac{\alpha}{m} \sum_{j=1}^m \ell(\theta, Y_j^*)$$
(4.2)

Define the generalized information matrix  $I:\Theta\to\mathbb{R}^{p\times p}$  by

$$I(\theta) = I_1(\theta) + \gamma I_2(\theta)$$

where

$$I_1(\theta) = \int \nabla \ell(\theta, Y) \nabla \ell(\theta, Y)^{\top} dF_0(Y), \qquad I_2(\theta) = \int \nabla \ell(\theta, Y) \nabla \ell(\theta, Y)^{\top} dF_{AI}(Y).$$

**Theorem 1.** Let  $\theta^*$  be the posterior bootstrap sample obtained from Algorithm 1 and denote with  $\Pi_{PB}$  its probability measure. For simplicity, consider the base measure  $F_{AI}$  to be atomic with m atoms<sup>2</sup>. Under regularity conditions, for any Borel set  $A \subset \Theta \subseteq \mathbb{R}^d$  with  $\alpha = \gamma n$  as  $n \to \infty$  we have

$$\Pi_{PB}\left[\sqrt{n(1+\gamma)}\left(\theta^* - \hat{\theta}_n^{\alpha}\right) \in A\right] \to P(z \in A)$$

 $\mathcal{D}_n$ -almost surely where  $\widehat{\theta}_n^{\alpha}$  is the empirical risk minimizer (4.2) and where  $z \sim N\left(0, J(\theta_0)^{-1}I(\theta_0)J(\theta_0)^{-1}\right)$  with  $J(\theta) = J_1(\theta) + \gamma J_2(\theta)$  and  $I(\theta) = I_1(\theta) + \gamma I_2(\theta)$  where (denoting  $\nabla$  the gradient operator with respect to  $\theta$ )

$$J_1(\theta) = \int \nabla^2 \ell(\theta, Y) dF_0(Y), \qquad J_2(\theta) = \int \nabla^2 \ell(\theta, Y) dF_{AI}(Y). \tag{4.3}$$

and

$$I_1(\theta) = \int \nabla \ell(\theta, Y) \nabla \ell(\theta, Y)^T dF_0(Y), \qquad I_2(\theta) = \int \nabla \ell(\theta, Y) \nabla \ell(\theta, Y)^T dF_{AI}(Y). \tag{4.4}$$

*Proof.* Appendix (See Section A.2). The result follow the same process as Theorem 1 in [26] whose proof hinges on Theorem 7 and Chapter 3 in [28] where all the regularity conditions are stated.

It it curious to compare the asymptotic distribution of posterior bootstrap and the Gibbs posterior (3.3). As noted earlier by [5] in the context of loss-likelihood bootstrap, the centering is the same but the covariance matrices are different when the loss function is not the usual log-likelihood in which case the bootstrap supplies the usual sandwich covariance matrix. The centering  $\hat{\theta}_n^{\alpha}$  of the asymptotic distribution may be a biased estimator of  $\theta_0$  when the prior influence does not vanish as  $n \to \infty$  (i.e. when  $\alpha = \gamma n$  and  $\gamma \ge 0$ ) and when the AI algorithm provides predictions that are systematically biased. Indeed, while in the parametric Bayesian framework the prior influence vanishes as  $n \to \infty$ , in Theorem 1 we allow for  $\alpha \to \infty$  yielding a possibly biased centering with the amount of bias determined by  $\gamma > 0$ . The prediction-powered inference framework [1, 2] estimates the severity of

<sup>&</sup>lt;sup>2</sup>When  $F_{AI}$  is absolutely continuous with respect to Lebesgue measure and we approximate it with a finite truncation of m samples, as in the posterior bootstrap algorithm, the same results hold but with  $F_{AI}$  replaced by the empirical distribution of the m drawn samples.

the bias on the labeled data  $\mathcal{D}_n$  by comparing observed labels  $Y_i$  to the AI-predicted ones  $\hat{\mu}(\boldsymbol{X}_i)$ . We could apply a de-biasing strategy similar to theirs in order to obtain a centering that is unbiased for  $\theta_0$ .

### 4.1 The Concentration Parameter $\alpha$

The concentration parameter  $\alpha > 0$  measures the assuredness of the prior about  $F_{AI}$  which can be interpreted as the effective sample size of the imaginary data  $\mathcal{D}_m^*$ . This can be seen from the characterization of the posterior in (3.7). While m is the actual sample size for  $\mathcal{D}_m^*$ , we treat it more as a truncation parameter in an approximation to the DP posterior where (similarly as for the catalytic priors in Section 2.1.3) the larger m is, the better. We can choose  $\alpha$  adaptively from out-of-sample experiments to determine the relevance of the AI non-parametric prior for prediction and to find the most suitable degree of AI prior subjectivity.

### 4.1.1 Calibration via Coverage

Another option is to choose  $\alpha$  in order to calibrate the coverage of posterior credible intervals in the frequentist sense. One way to do this would be via an adaptation of the general posterior calibration algorithm of [34]. Given access to mechanism to repeatedly accrue samples of size n from the data-generating process, as well as knowledge of a true parameter of interest  $\theta^*$ , one would be able to choose  $\alpha$  such that a  $1-\delta$  posterior credible interval arising from the  $\alpha$ -AI prior has frequentist coverage at level  $1-\delta$ . This would be approximated by repeatedly sampling datasets  $\mathcal{D}_n$ , computing the  $1-\delta$  credible region, and determining the proportion of times that the true parameter lies within. The practitioner would then want to choose the largest value of  $\alpha$  such that the  $1-\delta$  credible interval has frequentist coverage at level  $1-\delta$ , maximizing the informativeness of the prior under the constraint of well-calibrated posterior credible regions. Of course, practitioners do not have access to  $\theta^*$  or the ability to generate new data samples. Adapting the general posterior calibration algorithm [34], we can replace sampling independent datasets with bootstrapping datasets of size n from the empirical distribution of the actual sample  $\mathcal{D}_n$ . Similarly,

knowledge of  $\theta^*$  is replaced with the empirical risk minimizer on the bootstrapped dataset. One can then solve for  $\alpha$  using the same criterion—the largest value of  $\alpha$  such that the estimate of the coverage arising from the bootstrapped samples is at least  $1 - \delta$ .

### 4.1.2 Asymptotic Calibration

Adaptive tuning has been also considered in the context of prediction-powered inference by [2] who consider a weighted average of loss functions for estimating  $\theta_0$  with the weight chosen adaptively from data to minimize the Fisher information number, i.e. trace of the inverse asymptotic covariance matrix. This weight calibration is related to the one considered in [5] who calibrate a weight of the Gibbs posterior by matching the asymptotic covariance matrices of the Gibbs posterior and the loss-likelihood bootstrap. While these calibrations are ultimately asymptotic as  $n \to \infty$ , we could consider a similar strategy to find  $\alpha$  that minimizes the trace of an estimate of  $J(\theta_0)^{-1}$  in Theorem 1. This estimate could be obtained by replacing  $J_0(\cdot)$  and  $I_0(\cdot)$  with their finite-sample counterparts and replacing  $\theta_0$  with  $\hat{\theta}_n$ . Defining  $\hat{\Sigma}(\alpha)$  to be the estimate of the asymptotic covariance, this implicitly defines a function  $\alpha \mapsto \hat{\Sigma}(\alpha)$  which can be solved for  $\alpha$  when equated to a reasonable target. In many cases, such a target can be identified from the asymptotic marginal variances used to construct confidence intervals for the PPI estimator [1]. Indeed, defining  $\hat{\sigma}_{n,N,j}^2$  to be the jth component of the p-dimensional parameter of interest, we can solve the equation  $\operatorname{tr}\left(\hat{\Sigma}(\alpha)\right)^{-1} = \sum_{j=1}^{p} \hat{\sigma}_{n,N,j}^{2}$  to find a value of  $\alpha$  such that the size of the credible intervals are calibrated relative to PPI. In our experiments, we use both of the aforementioned strategies for eliciting values of  $\alpha$  for the DP prior, and generally find relatively compatible results (refer to Section 5.3).

We can calibrate the DP prior parameter  $\alpha$  via the asymptotic covariance in Theorem 1. Define  $\Sigma(\gamma) = J(\theta_0^{\gamma})^{-1}I(\theta_0^{\gamma})J(\theta_0^{\gamma})^{-1}$ . For any estimand  $\theta$  that is a convex risk minimizer, we let  $\Sigma_n^{PPI}$  be the asymptotic covariance for a sample of size n used to construct PPI confidence intervals [1]. In practice, the true risk minimizer  $\theta_0^{\gamma}$  as well as population quantities  $J(\theta_0^{\gamma}), I(\theta_0^{\gamma})$ , are not available. We can estimate the asymptotic covariance using

the empirical versions of the information matrices and the empirical risk minimizer as

$$\widehat{\Sigma}(\alpha) = J_n^{\alpha}(\widehat{\theta}_n^{\alpha})^{-1} I_n^{\alpha}(\widehat{\theta}_n^{\alpha}) J_n^{\alpha}(\widehat{\theta}_n^{\alpha})^{-1}.$$

Theorem C.1 of Angelopoulos et al. [1] provides an asymptotically valid confidence interval for the PPI estimator for estimands arising from nondegenerate convex optimization problems. For a p-dimensional estimated  $\theta^*$ , the theorem shows marginally that for each component j, we have, in their notation,

$$\sqrt{N}\left(\widehat{\Delta}_{\theta^*,j} + \widehat{g}_{\theta^*,j}^f - \mathbb{E}\left[\widehat{\Delta}_{\theta^*,j} - \mathbb{E}\left[\widehat{\Delta}_{\theta^*,j}\right]\right]\right) \stackrel{d}{\to} N\left(0, \frac{1}{p}\sigma_{\Delta,j}^2(\theta^*) + \sigma_{g,j}^2(\theta^*)\right).$$

Indeed, this asymptotic marginal variance can also be approximated by plugging in an estimate for  $\theta^*$ , and replace population quantities with their empirical versions.

We can proceed to calibrate our DP prior parameter  $\alpha$  by equating the trace of the estimated asymptotic covariance of our posterior bootstrap samples with the estimated asymptotic covariance that implicitly is used to construct the asymptotic PPI confidence interval. This yields the equation

$$\frac{\operatorname{tr}(\widehat{\Sigma}(\alpha))}{n+\alpha} = \sum_{j=1}^{p} \frac{\widehat{\sigma}_{\Delta,j}^{2}(\widehat{\theta})}{n} + \frac{\widehat{\sigma}_{g,j}^{2}(\widehat{\theta})}{m}$$

which can be solved in terms of  $\alpha$  via an iterative root-finding algorithm.

## 5 Generative AI Illustrations

We demonstrate our approach on two classification datasets, where generative AI input could be incorporated in predictive inference for medical diagnosis or parameter inference in labeling massive galaxy images.

### 5.1 Skin Disease Prediction

We apply our methodology towards the classification of Erythemato-Squamous diseases from descriptions of clinical symptoms. Erythemato-Squamous diseases (ESDs) comprise a group of six distinct but closely overlapping skin conditions that pose significant diagnostic challenges due to their similar clinical and histopathological features. Machine

learning approaches have been applied to predict the disease subtype from these clinical and histopathological features with high accuracy, additionally providing interpretable patterns [36]. This dataset has also been employed for exploring uncertainty quantification in large language model-based medical diagnosis. Kim et al. [24] used ChatGPT to diagnose ESDs from descriptions of clinical features only, applying conformal prediction techniques to aid in uncertainty quantification. Notably, ChatGPT's diagnoses from clinical symptoms only were less accurate than that of bespoke machine learning algorithms (i.e. a simple random forest model, for example), but still substantially better than random guessing.

ESDs are divided into the following six subtypes, which are the labels in this classification problem: psoriasis, seborrheic dermatitis, lichen planus, pityriasis rosea, chronic dermatitis and pityriasis rubra pilaris. There are twelve clinical features, ten of which are ordinal variables that take values in the set  $\{0,1,2,3\}$ , describing levels of prevalence. These features include things like redness, itchiness, or incidence in certain regions of the body. The other variables are family history (binary) and age (integer valued). Clinical features are those based on observable signs and symptoms that can be identified through physical examination and patient history, in contrast to histopathological features which are typically examined under a microscope after a biopsy.

Through our framework of generative AI priors, we leverage pre-trained large language models (ChatGPT) as complementary diagnostic tools to enhance the predictive capabilities of traditional machine learning systems at classifying skin disease diagnoses correctly.

#### 5.1.1 Data

We analyze the dermatology data<sup>3</sup> available from the UCI machine learning repository [21], removing histopathological features so as only to diagnose disease from clinical features. For this experiment, we split the total number of observations in the dataset (366) as follows: 20% is used as training data, treated as correctly labeled pairs. 20% is held-out to assess test accuracy. The remaining 60% is considered to be extra unlabeled data, for which the clinical symptoms are known to the practitioner but the labels are not. We let

<sup>&</sup>lt;sup>3</sup>Available at https://archive.ics.uci.edu/dataset/33/dermatology

 $\mathcal{D}_n$  denote the labeled training data,  $\mathcal{D}_T^{Test}$  the labeled testing data and denote the extra unlabeled data as  $\mathcal{D}_m^*$ .

#### Prompting ChatGPT to Impute Diagnoses 5.1.2

As discussed in Section 3.2.1, the base measure  $F_{AI}$  for our AI prior is characterized by a probability distribution on both clinical features X and labels Y. In this case, we define such a base measure as follows: the marginal distribution of clinical features is from the empirical distribution of extra unlabeled data, that is,  $f_{AI}^X(\boldsymbol{X}^*) = \frac{1}{n} \sum_{i=1}^n \delta_{\boldsymbol{X}_i}(\boldsymbol{X}^*)$ . Then, the conditional AI prior on the labels is given by the GPT-imputed conditional distribution on the feature X using the strategy described below.

In order to convert use ChatGPT to predict labels (diagnoses) from clinical features, we first convert the set of features to a prompt. We elicit these responses from the GPT-40 language model, using a temperature setting of 0.7. For this experiment, we used prompts with the following general format<sup>4</sup>

**Prompt:** Predict the diagnosis of Erythemato-Squamous disease from the following clinical features. The age feature simply represents the age of the patient. Family history is a binary variable. Every other feature was given a degree in the range of 0 to 3. Here, 0 indicates that the feature was not present, 3 indicates the largest amount possible, and 1, 2 indicate the relative intermediate values.

erythema: 2, scaling: 2, itching: 3, [...], age: 55
[...] Estimate the probability of each possible diagnosis for this case [...]

GPT-4o: psoriasis: 0.45, lichen planus: 0.20, [...]

We parse the textual response into a probability distribution on classes using regular expressions. We employ an additional normalizing step to ensure the given probabilities sum to one, though it is almost never necessary. We take the class with largest probability as the AI-predicted label, breaking ties uniformly at random if necessary.

<sup>&</sup>lt;sup>4</sup>The prompt shown here is slightly simplified, excluding instructions on how to format the output. We give the exact verbatim prompt in Section A.1.

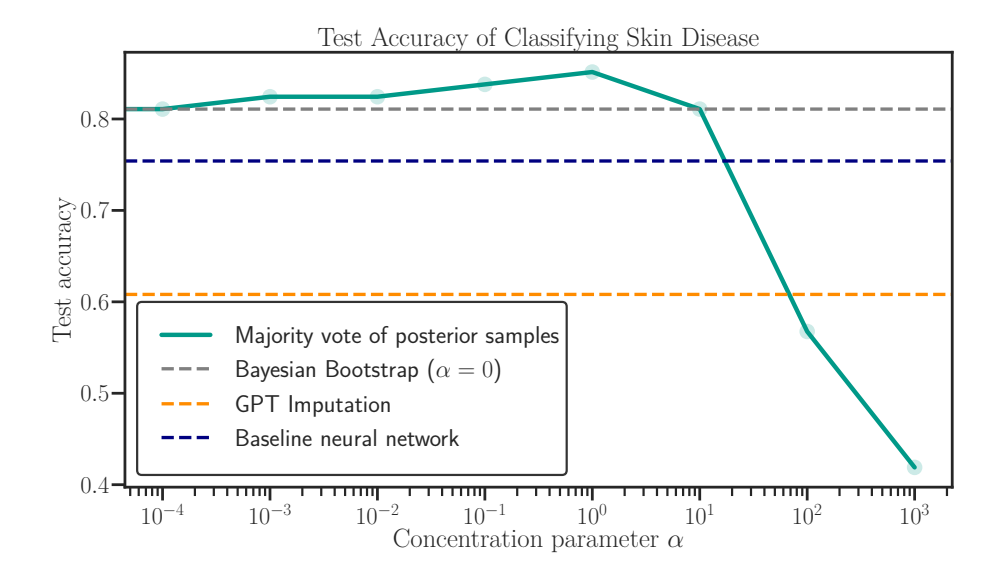


Figure 1: Classification accuracy of ESD on held-out test data, using a neural network trained on n = 58 observations. The line indicates mean performance after 10 repetitions. Horizontal lines indicate the test performance of a fitted neural network fit on training data only, and ChatGPT imputations.

#### 5.1.3 Non-parametric AI Bayesian Inference

For this data, we posit a parametric model for the conditional probabilities of each label via a three-layer neural-network parameterized vector function  $f_{\theta}: \mathcal{X} \to \mathcal{S}^{6}$ , where  $\mathcal{S}^{6}:=\{v \in \mathbb{R}^{6}: \sum_{i=1}^{6} v_{i}=1, v_{i} \geq 0 \,\forall i=1,\ldots,6\}$  denotes the simplex on 6-elements. The architecture of the neural network is rather uncomplicated and is described below.

The neural network parameterizes a class of functions  $f_{\theta}: \mathcal{X} \to \mathcal{S}^K$  through the following function composition

$$f_{\theta} = \operatorname{softmax} \circ f_{\mathbf{W}_3, \mathbf{b}_3} \circ \sigma \circ f_{\mathbf{W}_2, \mathbf{b}_2} \circ \sigma \circ f_{\mathbf{W}_1, \mathbf{b}_1}$$

where  $\theta = (\mathbf{W}_1, \mathbf{b}_1, \mathbf{W}_2, \mathbf{b}_2, \mathbf{W}_3, \mathbf{b}_3)'$ , and  $\mathbf{W}_1 \in \mathbb{R}^{64 \times 12}, \mathbf{b}_1 \in \mathbb{R}^{64}, \mathbf{W}_2 \in \mathbb{R}^{32 \times 64}, \mathbf{b}_2 \in \mathbb{R}^{32},$  $\mathbf{W}_3 \in \mathbb{R}^{6 \times 32}, \mathbf{b}_3 \in \mathbb{R}^6$ . In addition,  $\sigma$  denotes the ReLU activation function  $\sigma(x) = \max\{0, x\}, f_{W,b}$  denotes the affine transformation  $f_{\mathbf{W},b}(x) = \mathbf{W}x + \mathbf{b}$ , and softmax is defined via

$$\operatorname{softmax}(\mathbf{z})_i = \frac{\exp(z_i)}{\sum_{j=1}^6 \exp(z_j)}.$$

The neural network parameters are fit using the Adam optimizer to minimize the weighted cross-entropy loss, with a learning rate of 0.001. We also employ dropout with p = 0.2 during training. The clinical symptom covariates are first preprocessed by standardizing the age feature (by subtracting its mean and dividing by the unbiased estimate of its standard deviation).

Our inferential target is the minimizer of the induced empirical classification loss on the neural network weights  $\theta$ . The Posterior Bootstrap distribution  $\{\theta^{(t)}\}_{t=1}^{B}$  obtained from Algorithm 1 induces a posterior distribution on  $f_{\theta}(\cdot)$  and thereby also posterior predictive distribution on the label  $Y_{j}$  corresponding to test data  $\mathbf{X}_{j} \in \mathcal{D}_{T}^{Test}$  for  $1 \leq j \leq T$ . The final prediction of the label will be the majority vote

$$\widehat{Y}_{j} = \arg \max_{c \in \{1, \dots, 6\}} \frac{1}{B} \sum_{t=1}^{B} f_{\theta^{(t)}}^{c}(\boldsymbol{X}_{j})$$
(5.1)

where  $f_{\theta^{(t)}}^c(\cdot) = P[Y=1 \mid \theta^{(t)}, \cdot]$ . We evaluate the performance of this classification rule through the estimated misclassification rate  $P[Y_j \neq \hat{Y}_j]$  from T out-of-sample observations.

We approximately sample B=100 samples from the posterior predictive distribution on the label of each held-out test observation using the posterior bootstrap algorithm, using a truncation size of m=100. This essentially materializes as the following: for each posterior sample  $t=1,\ldots,B$ , we fit the neural network using a weighted loss induced by the AI prior, and classify each test point using (5.1). We fit the neural network using the Adam optimizer with a finite maximum number of epochs, which we note adds an additional degree of approximation to the posterior sampling procedure.

We employ this procedure for a range of  $\alpha$  values (the concentration parameter in the Dirichlet Process AI prior discussed in Section 4.1), and repeat it for ten repetitions. Figure 1 displays the average out-of-sample classification accuracy as a function of the concentration parameter  $\alpha$ . The blue dashed horizontal line indicates the classification accuracy of a classification rule  $\hat{Y}_{j,DL} = \arg\max_{c \in \{1,\dots,6\}} f_{\hat{\theta}}^c(\boldsymbol{X}_j)$ , where  $\hat{\theta}$  has been estimated purely on the training data. Due to stochasticity in predictions from the optimization procedure (see Section 5.1.3), the line indicates the average accuracy over ten such estimations of  $\hat{\theta}$ . Employing our specified ChatGPT-powered AI prior, we see that a range of relatively small  $\alpha$  values leads to posterior predictive distributions that are more accurate

than predictions that arise when simply excluding the additional unlabeled data.

Interestingly, we note in this case that for  $\alpha > 10$ , the classification accuracy is diminished by the AI prior. Since  $\alpha$  can be interpreted as an effective sample size, this means that when we have more than  $\approx 18\%$  fake observations, the performance worsens. As shown in Figure 1, the baseline performance of ChatGPT imputations, computed as the average accuracy taken over ten repetitions using GPT-40 to classify each test point. That is, we repeat the following procedure ten times: impute  $\hat{Y}_j = \hat{\mu}(\boldsymbol{X}_j)$  for each test point indexed by j and compute the test accuracy. hovers at around 60% classification accuracy, and the majority vote accuracy of the AI posterior shrinks to this level as  $\alpha$  grows towards the value of n=58. As  $\alpha$  becomes much larger than n, the performance further degrades. This indicates that predictive Bayesian analysis based on augmented data consisting of more imaginary than observed values does worse than baseline ChatGPT point predictions. The gray dashed line in Figure 1 indicates the performance for  $\alpha = 0$ , where the procedure boils down to the Bayesian bootstrap (Algorithm 2 in [26]) where we obtain uncertainty quantification based on only  $\mathcal{D}_n$ . The best out-of-sample prediction error was achieved for  $\alpha = 1.0$  which yielded a 5% increase in prediction accuracy over a procedure that does not use the fake data (with  $\alpha = 0$ ). This increase is notable as the AI predictions themselves are not of significantly high quality.

### 5.2 Proportion of Spiral Galaxies

Prior work has collected human annotations of galaxy morphologies through the Galaxy Zoo 2 citizen science initiative [37], which contains over 1.3 million labeled images from the Sloan Digital Sky Survey. Angelopoulos et al. [1] estimate the proportion of galaxies exhibiting spiral arm features, which is useful for understanding stellar evolution and star formation. The setting is that the practitioner has access to a small number  $n \leq 1000$  of human-labeled data (galaxy images pair with human annotations), and a large quantity  $N \approx 1.5 \times 10^4$  of unlabeled galaxy images. A computer vision model is leveraged to impute the labels of these data points. For the sake of our experiment, we have access to the true labels of the N data points as well, which we additionally use to estimate  $\theta^* \approx 0.26$  as

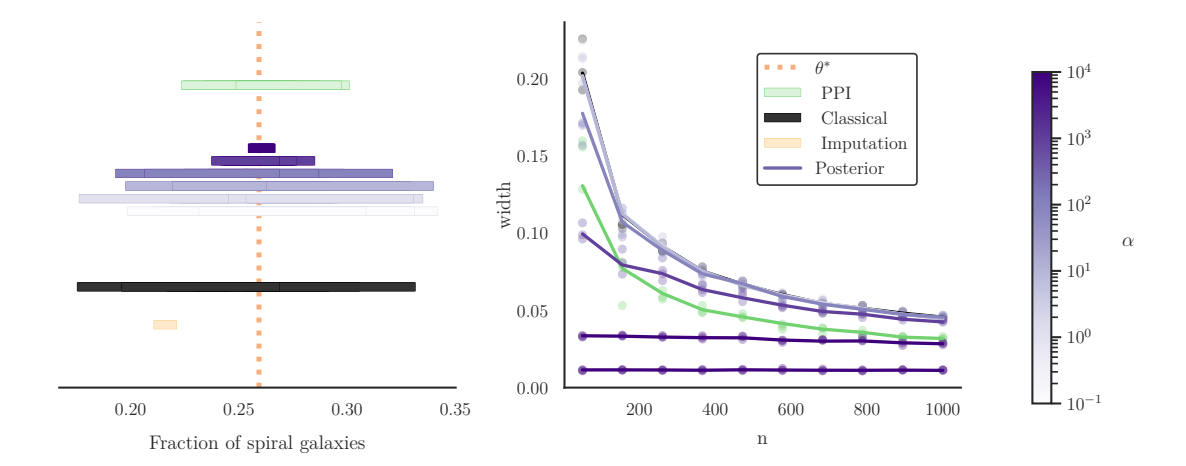


Figure 2: 90% Credible intervals for estimating the proportion of spiral galaxies. The left plot visualizes a credible interval from our method, compared with 90% confidence intervals around the classical and PPI estimator. The orange bar displays a confidence interval around the classical estimator when all imputed data is treated as real data. The right plot displays the width of credible/confidence intervals as a function of the labeled training data size n.

the "true mean proportion of spiral galaxies. However, we use knowledge of  $\theta^*$  purely for validation, and do not use it nor the true labels of the N computer-vision imputed data points for our analysis.

We adapt this setting to our AI prior framework, seeking to estimate the proportion of spiral galaxies in the universe. However, rather than using the AI-generated labels on additional data to debias an estimator [1], we perform a Bayesian inference on the unknown proportion of spiral galaxies leveraging the AI-predictions to elicit our prior knowledge.

#### 5.2.1 AI Priors on the Proportion of Spiral Galaxies

Suppose we have galaxy images  $X_1, \ldots, X_n$  with human annotations of their spirality  $Y_1, \ldots, Y_n$ . Additionally, we have unlabeled galaxy images  $X_1^*, \ldots, X_N^*$  with imputed labels  $Y_1^*, \ldots, Y_N^*$  produced via a large computer vision model. We take the nonparametric approach in Section 3.2 and define an AI base measure  $F_{AI}$  by the empirical distribution on the labels  $Y_1^*, \ldots, Y_N^*$  imputed by the computer vision model. This means that we do

not have an underlying continuous base measure and can do an exact algorithm without refreshing the labels for a fixed sub-sample of size m. We elicit our AI prior in turn as previously, via  $F \sim \mathrm{DP}(\alpha, F_{AI})$  where  $F_{AI}$  is now finitely supported on  $Y_j^*$ 's. We still use the approximate algorithm in Algorithm 1 using truncation  $m = 10^5$ , resampling from the empirical distribution of the atoms that make up the AI base measure here (the set of computer vision-imputed labels).

### 5.2.2 Nonparametric AI Inference on the Mean

Our inferential conclusions on the proportion of spiral galaxies stem from the posterior on the risk minimizer  $\theta(F)$ , defined via  $\theta(F) = \arg\min_{\theta} \int (y-\theta) \, \mathrm{d}F(y)$ . We obtain B=1000 samples from the approximate posterior distribution of  $\theta(F)$  using the exact variant of the posterior bootstrap algorithm in Algorithm 1. We repeat this procedure 10 times each for various values of the DP concentration parameter  $\alpha$  in the AI prior. Figure 2 displays the sizes of a single 90% credible interval for varying  $\alpha$  values, as well as the size of the 90% confidence interval for the classical sample mean (using only the human labeled data), the PPI estimator, and the sample mean when treating the imputed labels as real. The right hand side of the plot also visualizes the size of these confidence/credible intervals as the sample size n of human labeled data increases.

The posterior distribution on the proportion of spiral galaxies which arises from our AI prior obtains tight 90% credible intervals that concentrate around the mean. As  $\alpha$  grows larger, the predictions from the computer vision model become more heavily incorporated.

### 5.2.3 Calibrating the Concentration Parameter

The practitioner may also consider wish to consider choosing  $\alpha$  such that posterior credible regions are well-calibrated in a frequentist sense. Figure 3 displays the frequentist coverage of 90% posterior credible intervals around the mean (0.05 to 0.95 posterior quantiles). In order to gain the most from the AI prior while maintaining calibration, we can consider choosing the largest  $\alpha$  such that the credible interval stays well-calibrated. Credible intervals are constructed using the AI priors in Section 5.2.1, conditioning on n = 1000 data

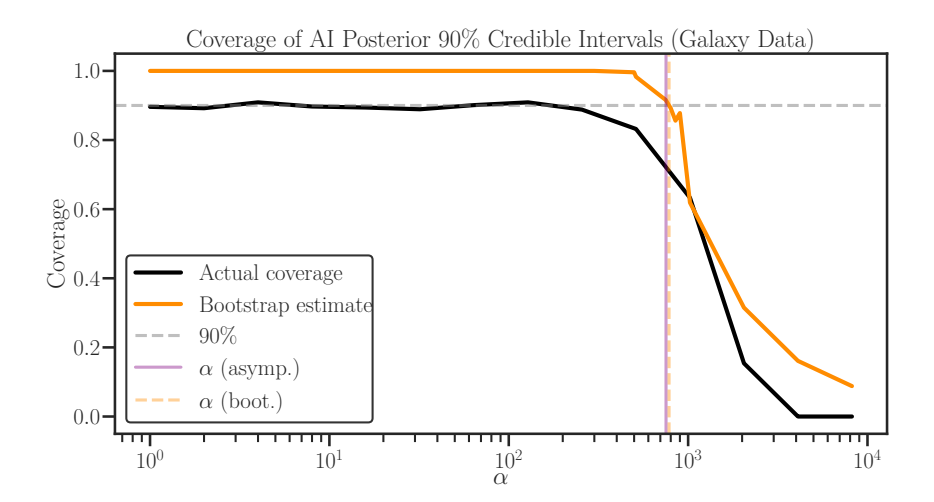


Figure 3: Frequentist coverage of AI posterior 90% credible intervals for the proportion of spiral galaxies. Intervals are from the 0.05 to 0.95 posterior quantile, using n = 1000 samples in the analysis, and the AI prior described in Section 5.2.1. We display the actual coverage computed using oracle knowledge, and a bootstrapped estimated of the coverage computable via sample information only. Vertical lines denote possible choices of  $\alpha$ .

points. Actual coverage is calculated from the proportion of intervals containing the true proportion of spiral galaxies  $\theta^* \approx 0.26$ , which in this case is taken to be the mean from the entire set of 16,743 labels available (see Section 5.2). The actual coverage (black line) in Figure 3 requires the ability to sample new datasets as well as oracle knowledge of the true parameter  $\theta^*$ . The bootstrap estimate of the coverage (orange line) is computed by bootstrapping samples from the empirical distribution of the 1000 labeled data points, and computing the proportion of times that the mean of this bootstrapped sample lies inside the interval. This procedure is similar to that in [34] and may be used to approximately calibrate posterior credible regions in absence of the knowledge of the true parameter. In this experiment, the largest  $\alpha$  value at which the posterior 90% credible interval is well-calibrated in the frequentist sense occurs approximately at  $\alpha = 200$ . Asymptotic covariance matching to PPI yields the value  $\alpha = 753$ , while the bootstrapping calibration algorithm yields the value  $\alpha = 783$ . The average width of the credible interval when the AI prior has this concentration parameter value of  $\alpha = 500$  is about 0.030, which is very similar to the

width of the 90% confidence interval around the PPI estimator.

### 5.3 Additional Experiments

We repeat our experimental procedure on six experiments studied in Angelopoulos et al. [1]. The data was obtained via the ppi-python package. Please refer to this work or the references therein for further information regarding any of these datasets. We provide any relevant details and experimental hyperparameters for each dataset below.

Each experiment follows the setup in prediction-powered inference, in which we have n labeled datapoints, and N unlabeled AI-imputed datapoints. In our case, we refine these N unlabeled datapoints into an AI prior by setting the base measure  $F_{AI}$  of our DP prior to be given by their empirical distribution.

For the optimization in each posterior bootstrap iteration, we optimize numerically using the L-BGFS solver. For each method, we obtain B=1000 samples using the posterior bootstrap algorithm. We construct a 90% credible interval from these set of samples by taking the 0.05 and 0.95 quantiles respectively as endpoints. We repeat each experiment varying over a range of n, and  $\alpha$  values (where  $\alpha$  is the DP prior parameter). We also repeat the experiment for a varying number of repetitions for each combination, so that we can assess variation and compute empirical coverage of the credible intervals. In each repetition, the n labeled datapoints are resampled from a larger body of available data.

Figure 4 displays the results regarding 90% posterior credible intervals for the parameter of interest using AI priors. In the leftmost column, we show the resulting interval widths for two choices of the DP prior parameter  $\alpha$ . In purple,  $\alpha$  was obtained by matching the asymptotic covariance to match that of PPI. In orange, we choose  $\alpha$  via the empirical calibration strategy derived from that used for Gibbs posteriors proposed by Syring and Martin [34]. We conclude that across our experiments, leveraging machine learning predictions via AI priors allows us to earn a concentration in posterior mass around the true parameter value. In the second column, we fix the value of n to be the largest that was analyzed for each dataset. We show the size of the 90% credible interval as a function of  $\alpha$ . Similarly, in the last column, we visualize the empirical coverage computed as the

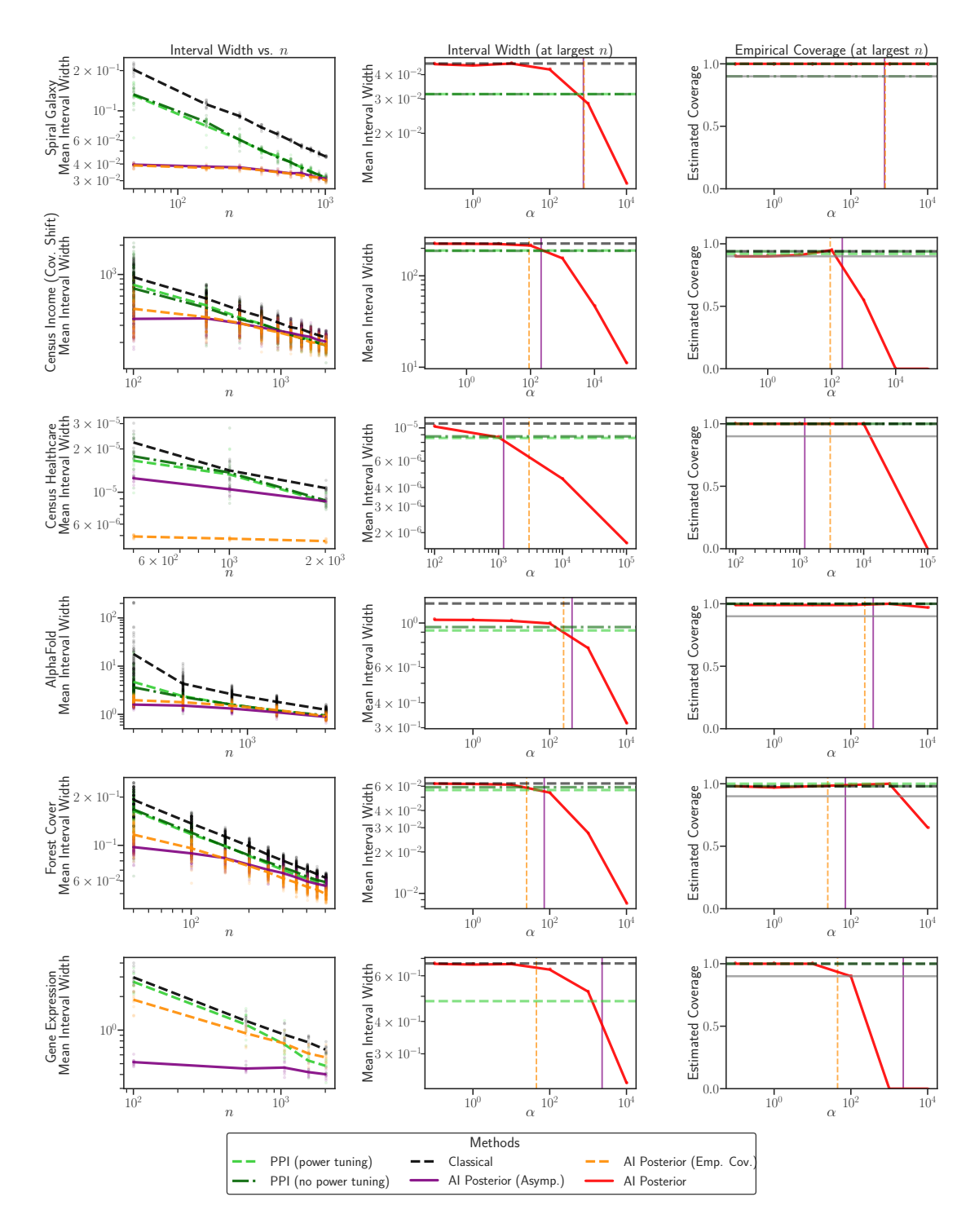


Figure 4: Interval width and coverage of AI posterior credible intervals on experiments from Angelopoulos et al. [1]. Left: size of the AI posterior credible interval for specific  $\alpha$  choices as a function of n. Middle: interval width as a function of  $\alpha$ . Right: empirical coverage of the intervals as a function of  $\alpha$ .

proportion of repetitions in which the true parameter falls into the interval. We note that this estimation may not be accurate for some of our experiments where only ten repetitions were performed.

**AlphaFold.** We construct a credible interval for the odds ratio based on credible intervals for the mean in each group, using the transformation used in [1]. We use values  $n \in \{200, 400, 800, 1500, 3000\}$  and perform 100 repetitions.

Census Healthcare. The parameter of interest is the logistic regression coefficient. We sample from the AI posterior using the posterior bootstrap algorithm minimizing the binary cross-entropy loss. We use values  $n \in \{500, 1000, 2000\}$  and perform 10 repetitions.

Census Income (covariate shift). The parameter of interest is the ordinary least squares regression coefficient in the covariate shifted population. We sample from the AI posterior using the posterior bootstrap algorithm minimizing the weighted least-squares loss. We use  $n \in \{10, 100, 2000\}$  and perform 100 repetitions.

**Spiral Galaxies.** The parameter of interest is the mean of binary data. This example is described in detail in Section 5. We use  $n \in \{10, 50, 1000\}$  and perform 10 repetitions.

Forest Cover. This experiment is carried out exactly as in the spiral galaxy data, as we are interested in the mean of binary data. We use  $n \in \{10, 50, 500\}$  and perform 100 repetitions.

**Gene Expression.** The parameter of interest is the 0.5 quantile (also known as the median). We use the posterior bootstrap minimizing the absolute error. We use  $n \in \{5, 100, 2000\}$  and perform 10 repetitions.

### 6 Discussion

This research note proposes a Bayesian alternative to prediction-powered inference framework introduced by [1] for performing valid statistical inference when an experimental dataset is augmented with predictions from an AI system. Our approach is based on prior construction based on simulations from an auxiliary black-box model. Our framework enables uncertainty quantification through non-parametric posteriors by viewing the machine learning system as a simulator from a prior on the unknown distribution function. Treating the generative black-box model as a base measure in the Dirichlet process prior  $DP(\alpha, F_{AI})$ , we achieve fully Bayesian inference about various quantities of interest (parameters associated with statistical models, parameters defined as minimizers of loss functions) using non-parametric posteriors. These posteriors give rise to posterior predictive distributions in parametric models which can be leveraged for decision making based on both AI input as well as observed data. We estimate the concentration parameter  $\alpha \geq 0$  from out-of-sample experiments to determine the inferential usefulness of AI predictions. The estimated value at  $\alpha = 0$  would signify that AI predictions do not add value and one is better off proceeding without them. We find that Bayesian analysis can be meaningfully enhanced with generative AI predictions on two real examples. We found that while AI predictions should not be taken literally for decision making, they can serve as a useful proxy (prior) for the correct answer which could enhance Bayesian analysis of observed data.

### References

- [1] Angelopoulos, A. N., S. Bates, C. Fannjiang, M. I. Jordan, and T. Zrnic (2023). Prediction-powered inference. *Science* 380(6649), 423–429.
- [2] Angelopoulos, A. N., J. C. Duchi, and T. Zrnic (2023). PPI++: Efficient prediction-powered inference. arXiv preprint arXiv:2311.01453.
- [3] Bedrick, E. J., R. Christensen, and W. Johnson (1996). A new perspective on priors

- for generalized linear models. Journal of the American Statistical Association 91 (436), 1450–1460.
- [4] Berger, J. O. and L. R. Pericchi (1996). The intrinsic Bayes factor for model selection and prediction. *Journal of the American Statistical Association* 91(433), 109–122.
- [5] Bissiri, P. G., C. Holmes, and S. G. Walker (2016). A general framework for updating belief distributions. *Journal of the Royal Statistical Society: Series B (Statistical Methodology)* 78(5), 1103–1130.
- [6] Chamberlain, G. and G. W. Imbens (1996). Nonparametric applications of Bayesian inference. *Journal of the American Statistical Association* 91(434), 124–135.
- [7] Chen, M.-H. and J. G. Ibrahim (2003). Conjugate priors for generalized linear models. Statistica Sinica 13(2), 461–476.
- [8] Chernozhukov, V. and H. Hong (2003, August). An mcmc approach to classical estimation. *Journal of Econometrics* 115(2), 293–346.
- [9] Dawid, A. (1992). Prequential data analysis. In *Current Issues in Statistical Inference:* Essays in Honor of D. Basu, pp. 113–126. Institute of Mathematical Statistics.
- [10] Diaconis, P. and B. Ylvisaker (1979). Conjugate priors for exponential families. *Annals of Statistics* 7(2), 269–281.
- [11] Ferguson, T. S. (1973). A Bayesian analysis of some nonparametric problems. *The Annals of Statistics* 1(2), 209–230.
- [12] Fong, E., C. Holmes, and S. G. Walker (2023). Martingale posterior distributions. Journal of the Royal Statistical Society: Series B (Statistical Methodology) 85(5), 1357–1378.
- [13] Fong, E., S. Lyddon, and C. Holmes (2019). Scalable nonparametric sampling from multimodal posteriors with the posterior bootstrap. In *Proceedings of the 36th International Conference on Machine Learning*, pp. 1952–1962. PMLR.

- [14] Fouskakis, D. and I. Ntzoufras (2016). Power-conditional-expected priors: Using gpriors with random imaginary data for variable selection. *Journal of Computational and* Graphical Statistics 25(2), 451–466.
- [15] Fouskakis, D., I. Ntzoufras, and K. Perrakis (2018). Power-expected-posterior priors for generalized linear models. *Bayesian Analysis* 13(3), 721–748.
- [16] Gelfand, A. E., D. K. Dey, and H. Chang (1992). Model determination using predictive distributions with implementation via sampling-based methods. In J. M. Bernardo, J. O. Berger, A. P. Dawid, and A. F. M. Smith (Eds.), *Bayesian Statistics* 4, pp. 147–167.
- [17] Good, I. J. (1983). Good Thinking: The Foundations of Probability and Its Applications. Dover Publications. Originally published in 1983 by the University of Minnesota Press.
- [18] Greenland, S. and R. Christensen (2001). Data augmentation priors for Bayesian and semi-Bayes analyses of conditional-logistic and proportional-hazards regression. *Statistics in Medicine* 20(16), 2421–2428.
- [19] Huang, D., N. Stein, D. B. Rubin, and S. C. Kou (2020). Catalytic prior distributions with application to generalized linear models. *Proceedings of the National Academy of Sciences* 117(20), 12004–12010.
- [20] Ibrahim, J. G. and M.-H. Chen (2000). Power prior distributions for regression models. Statistical Science 15(1), 46–60.
- [21] Ilter, N. and H. Guvenir (1998). Dermatology. UCI Machine Learning Repository. DOI: https://doi.org/10.24432/C5FK5P.
- [22] Ji, W., L. Lei, and T. Zrnic (2025). Predictions as surrogates: Revisiting surrogate outcomes in the age of AI. arXiv:2501.09731.
- [23] Kaji, T. and V. Ročková (2023). Metropolis-Hastings via classification. *Journal of the American Statistical Association* 118(544), 2533–2547.

- [24] Kim, J., S. O'Hagan, and V. Ročková (2024). Adaptive uncertainty quantification for generative AI. arXiv:2408.08990.
- [25] Laud, P. W. and J. G. Ibrahim (1996). Predictive specification of prior model probabilities in variable selection. *Biometrika* 83(2), 267–274.
- [26] Lyddon, S. P., C. C. Holmes, and S. G. Walker (2019). General Bayesian updating and the loss-likelihood bootstrap. *Biometrika* 106(2), 465–478.
- [27] Neal, R. M. (2001). Transferring prior information between models using imaginary data. Technical Report 0108, Department of Statistics and Department of Computer Science, University of Toronto.
- [28] Newton, M. A. (1991). The Weighted Likelihood Bootstrap and an Algorithm for Prepivoting. Ph. D. thesis, University of Washington. PhD Dissertation.
- [29] Nie, L. and V. Ročková (2022a). Bayesian bootstrap spike-and-slab lasso. *Journal of the American Statistical Association* 117(539), 1115–1130.
- [30] Nie, L. and V. Ročková (2022b). Deep bootstrap for Bayesian inference. *Philosophical Transactions of the Royal Society A: Mathematical, Physical and Engineering Sciences* 380 (2223), 20220154.
- [31] O'Hagan, A. (1995). Fractional Bayes factors for model comparison. *Journal of the Royal Statistical Society: Series B (Methodological)* 57(1), 99–138.
- [32] Pérez, J. M. and J. O. Berger (2002). Expected-posterior prior distributions for model selection. *Biometrika* 89(3), 491–512.
- [33] Spiegelhalter, D. J. and A. F. M. Smith (1982). Bayes factors for linear and log-linear models with vague prior information. *Journal of the Royal Statistical Society: Series B* (Methodological) 44(3), 377–387.
- [34] Syring, N. and R. Martin (2018, 12). Calibrating general posterior credible regions. Biometrika 106(2), 479–486.

- [35] van der Vaart, A. W. (1998). Asymptotic Statistics. Cambridge Series in Statistical and Probabilistic Mathematics. Cambridge: Cambridge University Press.
- [36] Wang, Z., L. Chang, T. Shi, H. Hu, C. Wang, K. Lin, and J. Zhang (2025). Identifying diagnostic biomarkers for erythemato-squamous diseases using explainable machine learning. *Biomedical Signal Processing and Control* 100, 107101.
- [37] Willett, K. W., C. J. Lintott, S. P. Bamford, K. L. Masters, B. D. Simmons, K. R. V. Casteels, E. M. Edmondson, L. F. Fortson, S. Kaviraj, W. C. Keel, T. Melvin, R. C. Nichol, M. J. Raddick, K. Schawinski, R. J. Simpson, R. A. Skibba, A. M. Smith, and D. Thomas (2013, September). Galaxy Zoo 2: Detailed morphological classifications for 304,122 galaxies from the sloan digital sky survey. *Monthly Notices of the Royal Astronomical Society* 435(4), 2835–2860.
- [38] Zellner, A. (1986). On assessing prior distributions and Bayesian regression analysis with g-prior distributions. In P. K. Goel and A. Zellner (Eds.), *Basic Bayesian Inference and Decision Techniques: Essays in Honor of Bruno de Finetti*, pp. 233–243. Amsterdam.
- [39] Zrnic, T. and E. J. Candés (2024). Cross-prediction-powered inference. *Proceedings of the National Academy of Sciences* 121(22), e2322083121.

## A Appendix

### A.1 Prompting

The exact prompt used for the AI base measure in the skin disease experiment was as follows:

Predict the diagnosis of Eryhemato-Squamous disease in the following case,  $\hookrightarrow \text{using the following clinical features.} \ \text{The age feature simply}$   $\hookrightarrow \text{represents the age of}$ 

the patient. Family history is a binary variable. Every other feature  $\hookrightarrow$  was given a degree in the range of 0 to 3. Here, 0 indicates that  $\hookrightarrow$  the feature was not present, 3 indicates the largest amount  $\hookrightarrow$  possible, and 1, 2 indicate the relative intermediate values.

erythema: 2.0, scaling: 2.0, definite borders: 0.0, itching: 3.0, koebner

⇒phenomenon: 0.0, polygonal papules: 0.0, follicular papules: 0.0, oral

⇒mucosal involvement: 0.0, knee and elbow involvement: 1.0, scalp

⇒involvement: 0.0, family history: 0.0, age: 55.0

The possible classes are: psoriasis, seboreic dermatitis, lichen planus, 

→ pityriasis rosea, cronic dermatitis, pityriasis rubra pilaris.

Please estimate the probability of each possible diagnosis for this  $\hookrightarrow$  case. The following is for research purposes only. I understand  $\hookrightarrow$  that a real patient must see a qualified doctor with such a  $\hookrightarrow$  concern.

Format your answer as:
psoriasis: (prob),
seboreic dermatitis: (prob),

Do your best to provide an accurate answer strictly in this format, and  $\hookrightarrow$ do not include anything else in your response.

### A.2 Proof of Theorem 1

*Proof.* Define the weighted generalized score function by

$$\widetilde{S}_n^{\alpha} = \sum_{i=1}^n w_i \nabla \ell(\theta, Y_i) + \sum_{i=1}^m \widetilde{w}_j \nabla \ell(\theta, Y_j^*),$$

and similarly the weighted sample generalized information matrix by

$$\widetilde{J}_n^{\alpha}(\theta) = \sum_{i=1}^n w_i \nabla^2 \ell(\theta, Y_i) + \sum_{i=1}^m \widetilde{w}_i \nabla^2 \ell(\theta, Y_j^*).$$

where  $(w_1, \ldots, w_n, \widetilde{w}_1, \ldots, \widetilde{w}_m)' \sim \text{Dirichlet}(1, \ldots, 1, \alpha/m, \ldots, \alpha/m)$ . We first argue that  $(n+\alpha)^{1/2}\widetilde{S}_n^{\alpha}(\widehat{\theta}_n^{\alpha}) \stackrel{d}{\to} N(0, I(\theta_0^{\gamma}))$  using the Cramér-Wold device as follows. Let  $z \in \mathbb{R}^p$  with  $||z||_1 = 1$ , and define

$$t_{n,\alpha}(z) \equiv \sqrt{n+\alpha} z^{\top} \widetilde{S}_{n}^{\alpha}(\widehat{\theta}_{n}^{\alpha})$$

$$= \sqrt{n+\alpha} \sum_{k=1}^{p} z_{k} \left( \frac{\sum_{i=1}^{n} V_{i} g_{k}(\widehat{\theta}_{n}^{\alpha}, Y_{i}) + \sum_{j=1}^{m} \widetilde{V}_{j} g_{k}(\widehat{\theta}_{n}^{\alpha}, Y_{j}^{*})}{\sum_{i=1}^{n} V_{i} + \sum_{j=1}^{m} \widetilde{V}_{j}} \right)$$

where  $V_1, \ldots, V_n \stackrel{iid}{\sim} \operatorname{Exp}(1)$ ,  $\tilde{V}_1, \ldots, \tilde{V}_m \stackrel{iid}{\sim} \operatorname{Gam}(\alpha/m, 1)$ , and  $g_k(\theta', Y) \equiv \frac{\partial \ell(\theta, Y)}{\partial \theta_k}|_{\theta = \theta'}$ . This can be rewritten as

$$t_{n,\alpha}(z) = \frac{1}{(n+\alpha)^{-1} \sum_{i} V_i + \sum_{j} \widetilde{V}_j} \cdot \frac{\sum_{i=1}^n a_i V_i + \sum_{j=1}^m \widetilde{a}_j \widetilde{V}_j}{\sqrt{n+m}}$$

The first factor in the product converges almost surely to 1. Thus, it is sufficient to show that

$$t'_{n,\alpha}(z) = \frac{\sum_{i=1}^{n} a_i V_i + \sum_{j=1}^{m} \tilde{a}_j \tilde{V}_j}{\sqrt{n+m}}$$

converges in distribution to  $N(0, z^{\top}I(\theta_0^{\gamma})z)$ . Indeed, we appeal to the Lindeberg-Feller-Lévy CLT. The average variance of the random variables summated in the numerator is given by

$$\bar{\sigma}_{n,\alpha}^2 = (n+\alpha)^{-1} \left( \sum_{i=1}^n a_i^2 + \frac{\alpha}{m} \sum_{j=1}^m \tilde{a}_j^2 \right)$$

and the asymptotic variance is thus

$$z^{\top} \left( I_1(\theta_0^{\gamma}) + \gamma I_2(\theta_0^{\gamma}) \right) z$$
.

Therefore, we have  $\sqrt{n+\alpha}\,\widetilde{S}_n^\alpha(\widehat{\theta}_n^\alpha)\stackrel{d}{\to} N(0,I(\theta_0^\gamma).$ 

Assuming smoothness conditions [26, 28] hold, we can perform a Taylor expansion of the weighted score function around the empirical risk minimizer  $\hat{\theta}_n^{\alpha}$  as

$$\widetilde{S}_n^{\alpha}(\widehat{\theta}_n^{\alpha}) = (\widetilde{J}_n(\widehat{\theta}_n) - R_n)(\theta^* - \widehat{\theta}_n^{\alpha})$$

for a remainder term  $R_n$ . Following Lyddon et al. [26],  $\tilde{J}_n^{\alpha}(\hat{\theta}_n^{\alpha}) - R_n$  converges to  $J(\theta_0^{\gamma})$  and is invertible with high probability. Slutsky's theorem then yields the desired result, with asymptotic covariance given by  $J(\theta_0^{\gamma})^{-1}I(\theta_0^{\gamma})J(\theta_0^{\gamma})^{-1}$ .